GaN quantum dot superlattices grown by molecular beam epitaxy at high temperature

Tao Xu[a)]
Photonics Center, Boston University, Boston, Massachusetts 02215, USA and Department of Electrical and Computer Engineering, Boston University, Boston, Massachusetts 02215, USA

Lin Zhou
School of Materials, Arizona State University, Tempe, Arizona 85287, USA and Department of Physics, Arizona State University, Tempe, Arizona 85287, USA

Yiyi Wang, Ahmet S. Özcan, and K. F. Ludwig
Physics Department, Boston University, Boston, Massachusetts 02215, USA

David J. Smith
School of Materials, Arizona State University, Tempe, Arizona 85287, USA and Department of Physics, Arizona State University, Tempe, Arizona 85287, USA

T. D. Moustakas
Photonics Center, Boston University, Boston, Massachusetts 02215, USA and Department of Electrical and Computer Engineering, Boston University, Boston, Massachusetts 02215, USA

(Received 22 June 2007; accepted 14 August 2007; published online 11 October 2007)

In this paper, we report the growth of GaN quantum dot superlattices (QDSLs) with AlN barriers on (0001) sapphire substrates by molecular beam epitaxy at relatively high temperature (770 °C) using the modified Stranski-Krastanov growth mode. Observations with atomic force microscopy show that the height distribution of the dots depends strongly on the number of GaN monolayers (MLs) grown on the AlN barriers. Specifically, the height distribution consists of two Gaussian distributions (bimodal) for coverages of 3 or 4 ML, and becomes a single Gaussian distribution for 5 and 6 ML of coverage. Furthermore, the density of quantum dots increases with the degree of coverage and saturates at 2×10^{11} dots/cm^2. An increase in the number of stacks in the superlattice structure with 4 ML coverage also leads to a more pronounced bimodal height distribution. Electron microscopy observations indicate that the GaN QDs are truncated pyramids faceted along the $\{1\bar{1}03\}$ planes and suggest that larger dots are associated with threading dislocations which presumably provide low-energy nucleation sites. Transmission electron microscopy studies also indicate that most of the larger dots are nucleated next to edge-type dislocations, while most of the smaller dots are located in dislocation-free regions. These GaN QDSLs were also studied by grazing-incidence small angle x-ray scattering and grazing-incidence x-ray diffraction methods. The average lateral deviation and the vertical correlation length between QD positions for two successive layers were determined to be 1.4 nm and 190 nm, respectively. A GaN QD growth model is proposed to explain the phenomenon. © *2007 American Institute of Physics*. [DOI: 10.1063/1.2787155]

I. INTRODUCTION

Quantum dots (QDs) can be used as the active region of optoelectronic devices, such as light-emitting diodes (LEDs), lasers, modulators, and detectors. The challenges in the growth of GaN QDs lie in the development of methods to obtain dots with good size uniformity and high spatial density. Recently, there has been significant progress in control of GaN QD growth by molecular beam epitaxy (MBE) using the Stranski-Krastanov (SK) mode.[1–4] Adelmann *et al.*[1] studied GaN QD growth on AlN buffers under N-rich conditions at 730 °C. Under these conditions, QDs were formed in the presence of N_2 plasma. The GaN QD growth was also studied under Ga-rich conditions, a method referred to as the "modified SK mode."[2,3] The two-dimensional (2D) GaN film grown on AlN under Ga-rich conditions was spontaneously rearranged into three-dimensional (3D) islands when the excess Ga was allowed to desorb under vacuum. Furthermore, it has been reported[1] that the GaN QD density often saturates at about 10^{11} dots/cm^2. GaN quantum dot superlattices (QDSLs) can be used to increase spatial density in the vertical direction. Electron microscopy observations showed that wurtzite GaN QDs grown on AlN may be coherent and dislocation-free.[5]

GaN optoelectronic devices are usually grown by MBE at 750–800 °C. However, for most results reported in the literature, the growth temperature for GaN QDs was in the range of 650–750 °C. In order to develop GaN QDs for optoelectronic devices, it is necessary to obtain better understanding of GaN QD growth at higher temperatures. In this paper, we report the MBE growth of GaN/AlN QDSLs at 770 °C under slightly Ga-rich conditions, using the modified SK mode. Factors that influence the dot density and distribution such as the GaN coverage and the number of GaN QD

a)Electronic mail: taoxu77@gmail.com

 © 2007 American Institute of Physics

Downloaded 21 Oct 2008 to 128.197.27.9. Redistribution subject to AIP license or copyright; see http://jap.aip.org/jap/copyright.jsp

stacks in the superlattice were investigated. In order to examine the surface morphology, film structural information, correlation in the vertical direction, and strain relaxation, the GaN QD samples were investigated by atomic force microscopy (AFM), transmission electron microscopy (TEM), grazing-incidence small angle x-ray scattering (GISAXS), and grazing-incidence x-ray diffraction (GID).

II. EXPERIMENTAL METHODS

The GaN quantum dot samples were grown in a Varian Gen II molecular beam epitaxy system which used standard effusion cells for Ga and Al evaporation. An EPI rf plasma source was used to activate the molecular nitrogen, and sapphire wafers with *c*-plane orientation were used as substrates.[6] The sapphire substrates were nitridated at 870 °C for 1 h, followed by deposition of a 300-nm-thick AlN film grown under Al-rich conditions at the same temperature. The substrate temperature was then reduced to 770 °C for the GaN QDSL growth. The superlattice periods consisted of GaN QDs obtained by depositing several monolayers (MLs) of GaN, separated by 10–20 nm of AlN barriers. The growth rate for GaN in this study was about 0.3 ML/s. The GaN QDs were grown using the modified SK growth mode. In this mode, several MLs of GaN were deposited under Ga-rich conditions (Ga/N≈1.1), followed by evaporation of excess Ga in vacuum, and subsequent rearrangement of the 2D GaN layers into 3D GaN dots. The 2D to 3D transition was confirmed by transformation of the reflection high-energy electron diffraction (RHEED) pattern from streaky to spotty during growth interruption. After deposition of the last GaN QD layer, the sample was left in vacuum for 1 min before the substrate temperature was ramped down to 200 °C at 20 °C/min.

The surface dot density and height were evaluated using AFM (Digital Instruments D3100). Height distribution of the QDs was obtained by using the "Depth" command in the software program of the microscope. TEM observations were carried out on both plan-view and cross-sectional samples prepared by standard mechanical polishing and ion-beam thinning. Conventional diffraction-contrast images were obtained in bright-field imaging mode using two-beam diffraction conditions on a JEM-2000FX TEM operated at 200 keV. High-resolution phase-contrast images were recorded with a JEM-4000EX high-resolution transmission electron microscope (HRTEM) operated at 400 keV. Grazing-incidence surface-sensitive x-ray experiments[7] were performed on the beamline X21 of the National Synchrotron Light Source, at Brookhaven National Laboratory. The scattering intensity was collected by a 1D position sensitive detector (PSD) with 1 s time resolution mounted parallel to the sample surface. For the GISAXS scans, the exit angle was kept the same as the incidence angle. The angles were varied to scan $q_\perp$ (momentum transfer perpendicular to the surface) from approximately 0.27 to 2.7 nm^{-1}. The in-plane radial GID scans were performed along the GaN/AlN $[l0\bar{l}0]$ direction, which includes the angular range of the sapphire $(11\bar{2}0)$ peak, GaN $(10\bar{1}0)$ peak, and AlN $(10\bar{1}0)$ peak.

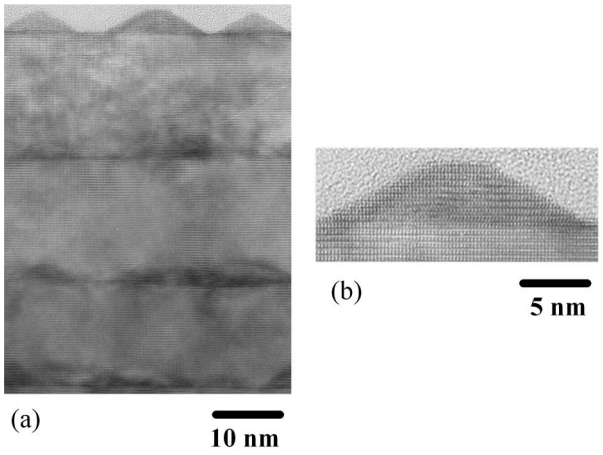

FIG. 1. (a) Cross-sectional TEM image of GaN QDSL sample with four stacks of QDs, grown with GaN coverage of Θ=5 ML; (b) High-resolution TEM image of GaN QD on surface of sample showing truncated pyramidal shape.

III. EXPERIMENTAL RESULTS AND DISCUSSION

A. Effect of GaN coverage

The GaN coverage (Θ), stated in monolayer (ML) units (where 1 ML=$c/2$=0.259 nm), is an important parameter directly affecting the evolution of GaN QDs during growth.[1] In this section, we describe the influence of GaN coverage on the QD height distribution, density, and microstructure for QDSL structures with four periods.

Figures 1(a) and 1(b) show the cross-sectional and high-resolution TEM images of a GaN QDSL structure, which consists of four stacks of GaN QDs obtained with 5 ML of GaN coverage, separated by 18 nm AlN barriers. From the electron micrographs, we estimate that the height of the QDs is about 4 nm and the dot diameter is about 15 nm. The QDs in the free surface have truncated pyramidal shapes, faceted along the $\{1\bar{1}03\}$ planes. The surface morphology of this GaN QDSL sample is also shown in the AFM height image of Fig. 2(a). The QD density on the top surface was measured to be 9×10^{10} cm^{-2}. The height distribution of the QDs, as shown in Fig. 2(b), has a Gaussian shape with an average height of 3.4 nm. Similar AFM analysis was carried out for samples produced at different GaN coverages as discussed below.

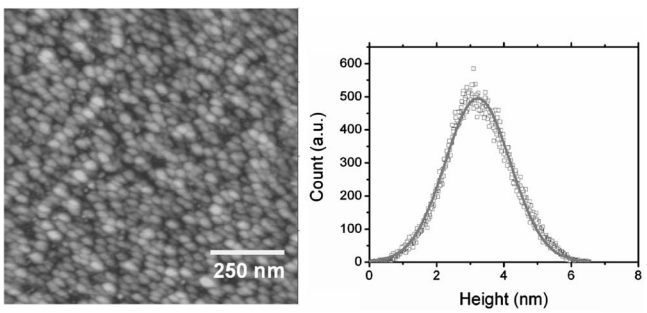

FIG. 2. (a) The 1×1 μm^2 AFM height image of GaN QDSL with four stacks of QDs and 5 ML GaN coverage in each stack (z scale is 10 nm); (b) height distribution of the top layer of dots shows Gaussian distribution.

Downloaded 21 Oct 2008 to 128.197.27.9. Redistribution subject to AIP license or copyright; see http://jap.aip.org/jap/copyright.jsp

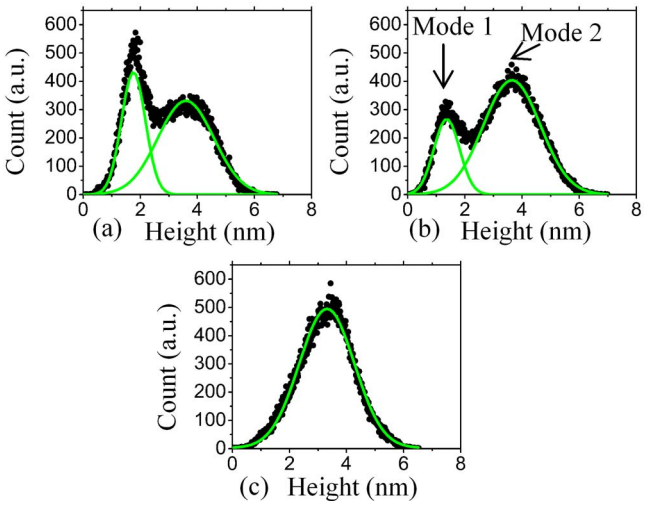

FIG. 3. (Color online) Dot height distribution for top layer of GaN QDSL samples of different GaN coverages (Θ): (a) Θ=3 ML; (b) Θ=4 ML; and (c) Θ=5 ML.

The height distributions of the surface QDs for samples produced with different GaN coverages are shown in Fig. 3. A clear bimodal distribution is visible in Figs. 3(a) and 3(b) for GaN coverage of 3 ML and 4 ML, respectively. Mode 1 has a narrow Gaussian distribution with an average height of about 1.4–1.8 nm and full width at half maximum (FWHM) of 0.8 nm. Mode 2 has a broader distribution with an average height of about 3.6 nm and FWHM of 2 nm. As the GaN coverage increases, mode 2 becomes more dominant. When the coverage is equal to or greater than 5 ML, the height distribution becomes practically Gaussian, with an average height of about 3.4 nm and FWHM of 1.8–1.9 nm, as shown in Fig. 3(c). Similar observations were reported in Ref. 1 on GaN/AlN QDs grown under N-rich conditions at 730 °C. It should be pointed out, however, that the 300 nm AlN film described in Ref. 1 was deposited on a 2-μm-thick metal-organic chemical vapor deposition (MOCVD)-grown GaN template. Thus the threading dislocation density of the sample in Ref. 1 is likely to be much lower (at least one order of magnitude) than for the AlN buffer layers in our current study, which were deposited directly onto (0001) sapphire substrates.

The dependence of GaN QD density on the GaN coverage is shown in Fig. 4. The total QD density increases with increasing GaN coverage and saturates at around $2\times10^{11}/\mathrm{cm}^2$ for 5 ML of GaN coverage. Moreover, the QD density for mode 1 decreased dramatically above 4 ML GaN coverage, as shown in Fig. 4(a). Figure 4(b) shows the ratio of mode 2 dot count to the total dot count for different GaN coverages. Mode 2 clearly becomes predominant with more GaN coverage.

B. Effect of the number of stacks

The strain field at the growth surface affects the location and shape of QDs. Self-aligned arrays of QDs have been reported for SL structures in the InAs/GaAs system,[8,9] and in the Ge/Si system.[10,11] In these two systems, the density of growth defects such as threading dislocations is very low

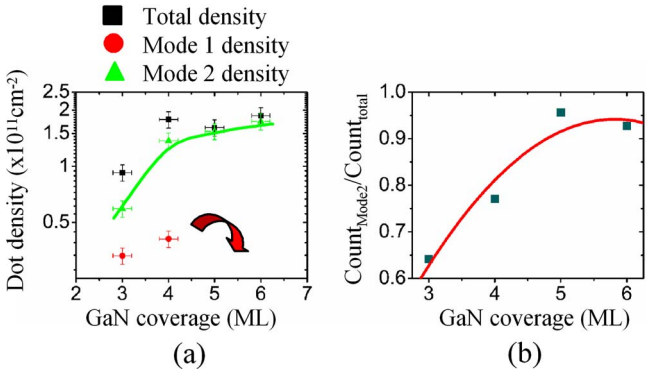

FIG. 4. (Color online) (a) Dependence of GaN QD density on GaN coverage for GaN QDSLs of four stacks; (b) ratio of mode 2 dot count to total dot count with respect to GaN coverage.

compared with the QD density, which is not the case for the GaN/AlN system. For a GaN QDSL, the strain field present during growth will be caused by buried layers as well as by threading dislocations that are present within the SL structure.[12] Three GaN QDSL samples with 1, 4, and 30 stacks were grown to compare the effect of the strain field in the GaN/AlN system. The AlN spacing layer thickness was fixed at ~10 nm, and the GaN coverage for each QD layer was 4 ML.

A cross-sectional TEM image for the GaN QDSL sample with 30 stacks is shown in Fig. 5. Some of the threading defects tend to annihilate as the number of stacks increased and there is significant vertical correlation of the dots, indicating the importance of the strain field caused by buried layers. Diffraction-contrast analysis was used to characterize the defects. Cross-section electron micrographs were recorded under two-beam diffraction conditions to enable the dislocation type to be identified using Burgers' vector analysis. The micrograph in Fig. 6(a) was taken with $g=(0002)$ to show screw ([0002])- and mixed-type dislocations, while the image in Fig. 6(b) was taken with $g=(10\bar{1}0)$ to show edge $(1/3[11\bar{2}0])$-type and mixed type dislocations. It was found that threading dislocations (TDs) with edge components were by far the most prevalent type of defects (>95%) in this sample.

The height distribution for the QDs on the top layers of these three different GaN/AlN QDSL samples is shown in

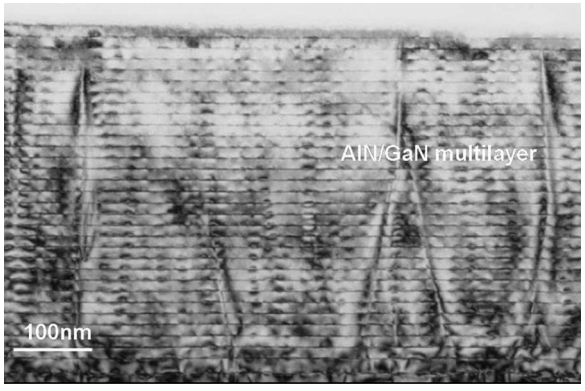

FIG. 5. Cross-sectional TEM image for 30-stack GaN/AlN QDSL sample with GaN coverage of Θ=4 ML in each stack.

Downloaded 21 Oct 2008 to 128.197.27.9. Redistribution subject to AIP license or copyright; see http://jap.aip.org/jap/copyright.jsp

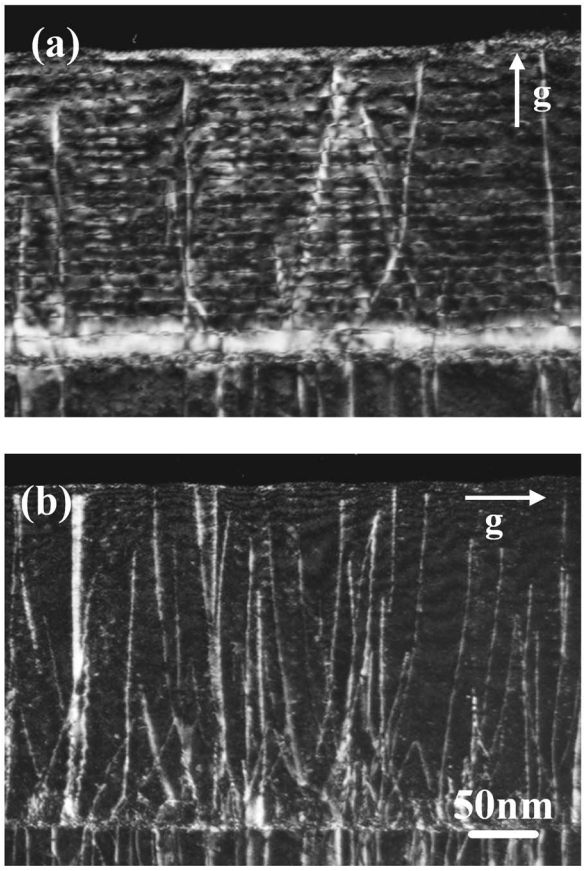

FIG. 6. Cross-section electron micrographs of GaN QDSL sample with 30 stacks taken under two-beam diffraction conditions to enable dislocation type to be identified using Burgers' vector analysis: (a) $g=(0002)$ and (b) $g=(10\bar{1}0)$; images (a) and (b) taken from almost same area. Image (a) shows some screw ([0002])- and mixed-type dislocations; image (b) shows some edge $(1/3[11\bar{2}0])$-type and mixed-type dislocations.

Fig. 7. The distribution is bimodal with mode 1 becoming progressively stronger as the number of stacks increases. For the sample having only one GaN stack, both modes 1 and 2 have smaller heights and their distributions are narrower compared to samples with 4 or 30 GaN stacks. This may be related to the difference in strain experienced by the GaN QDs in a single stack or multiple stacks. In a single stack, the growth of GaN QDs is affected by the lattice mismatch between AlN and GaN, while in multiple stacks, the growth of GaN QDs is affected by the strain associated with the AlN interlayers as well as by the buried GaN QDs.

The sample with 30 GaN stacks was also investigated by GISAXS in order to determine the degree of vertical alignment. Figure 8 shows the GISAXS profile for the 30-stack GaN QDSL sample. The well-defined Bragg sheets indicate a high degree of vertical alignment of the QDs. Their distance in reciprocal space is related to the bilayer thickness $T=2\pi/\Delta q_{\perp}$, which is ~18 nm. The broadening of the Bragg sheets along the $q_{\perp}$ direction as a function of $q_{\parallel}$ is related to the vertical misalignment of the QDs:[13]

$$\Delta q_{\perp}^{\mathrm{HWHM}} = \frac{\sigma^2}{T} q_{\parallel}^2 + \frac{\mu}{T}, \tag{1}$$

where $\Delta q_{\perp}^{\mathrm{HWHM}}$ is the half width at half maximum of the Bragg sheet in the $q_{\perp}$ direction, σ is the average lateral deviation between QD positions for two successive layers, and μ is the attenuation factor per layer, which is constant along the Bragg sheet. By plotting $\Delta q_{\perp}^{\mathrm{HWHM}}$ vs $q_{\parallel}$ from the third Bragg sheet in Fig. 8 and fitting the data with the expression in Eq. (1), the average lateral deviation σ is obtained to be approximately 1.4 nm. The vertical correlation length can be derived using the same expression: Vertical correlation length=dot base diameter/$\sigma\times T$. The calculation gives the vertical correlation length to be approximately 190 nm, using a dot base diameter of 15 nm estimated from the cross-sectional HRTEM images, as shown in Fig. 1(b).

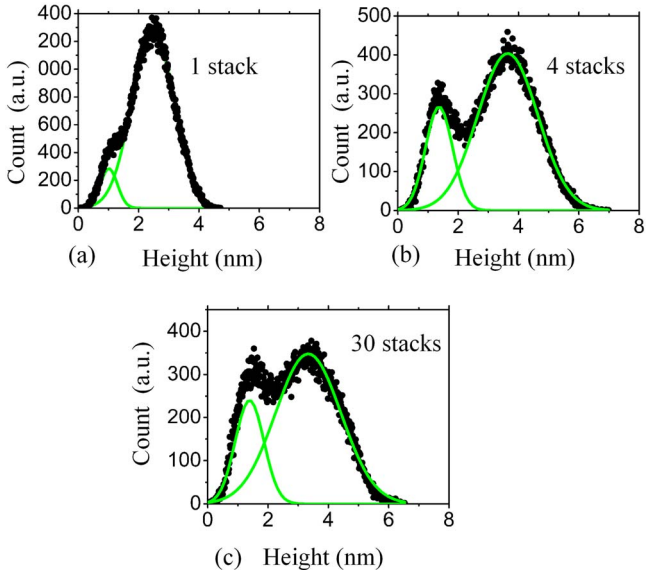

FIG. 7. (Color online) Height distribution of GaN/AlN QDSL samples for different numbers of stacks and same GaN coverage (Θ=4 ML) in each stack: (a) 1 stack, (b) 4 stacks, and (c) 30 stacks. The island height distributions for these samples clearly have bimodal distribution with mode 1 becoming progressively stronger with number of stacks.

Chamard *et al.*[14] studied 13-stack GaN QDSL sample grown on 6H-SiC(0001) wafer and found that the average lateral deviation and the vertical correlation length between QD positions for two successive layers were 0.66 nm and

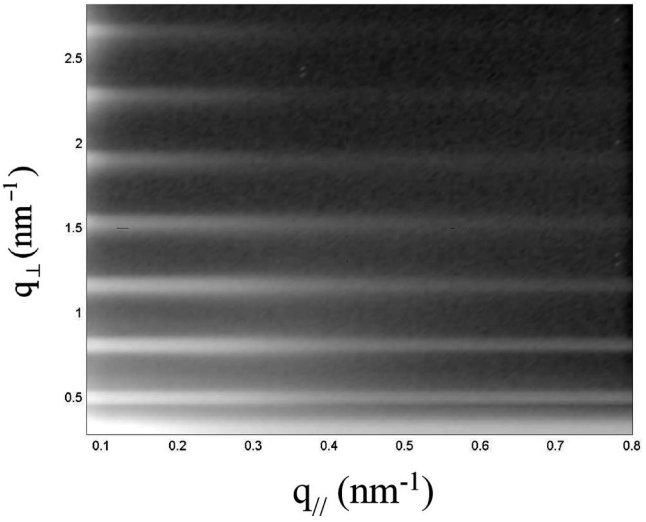

FIG. 8. GISAXS $q_{\perp}$ scan for the 30-stack GaN QDSL sample.

Downloaded 21 Oct 2008 to 128.197.27.9. Redistribution subject to AIP license or copyright; see http://jap.aip.org/jap/copyright.jsp

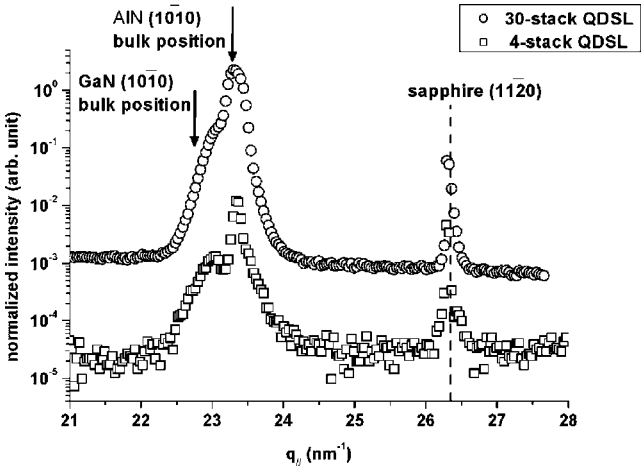

FIG. 9. The x-ray GID patterns for the 30-stack GaN QDSL sample (empty squares) and the 4-stack GaN QDSL sample (empty circles) in log scale along the GaN [$l0\bar{1}0$] direction at incident x-ray energy of 10.25 keV. The sapphire (11$\bar{2}$0) peak position is marked by dashed line.

150 nm, respectively. The larger average lateral deviation (σ=1.4 nm) derived in the current study may be due to the higher dislocation density in the AlN film.

Figure 9 shows the x-ray in-plane GID radial scans for the 30-stack and 4-stack GaN QDSL samples along the AlN [$l0\bar{1}0$] direction. The sapphire (11$\bar{2}$0) peaks are indicated by the dashed line. The larger peaks in the plot of each sample appear at similar $q_{\|}$ values for the bulk AlN position (pointed by arrow). These peaks could be diffracted from the AlN spacers, in which the strains are presumably fully relaxed. The peaks at the left side of AlN (10$\bar{1}$0) peaks have lattice mismatches approximately 1.34% and 1.58% with respect to AlN for the 30-stack and 4-stack samples, respectively. These could be the GaN (10$\bar{1}$0) peaks which are diffracted from the highly strained GaN QDs that are vertically correlated. Strain is more relaxed with respect to bulk GaN position for the 4-stack sample than that for the 30-stack sample.

Bright-field plan-view TEM images were used to determine the density of dislocations with edge components as well as to assess any correlation between dislocations and QDs. Figure 10(a) shows an image of the GaN QDSL sample with 30 GaN stacks. The patches of faint dark contrast correspond to the GaN QDs, while the small black spots correspond to dislocations having edge components. As shown in this plan-view TEM image, some GaN QDs are associated with threading dislocations while other QDs appear to be located in areas that are free of dislocations, as indicated by the arrows. Moreover, the GaN QDs associated with dislocations sometimes appear to have larger diameters than QDs located in the dislocation-free regions. Similar trends can be also observed in the cross-sectional TEM image of the same sample, as shown in Fig. 10(b). The GaN QDs associated with TDs seem to have larger height than those located away from the TDs. It seems possible that this trend could be connected to mode 2 and mode 1 QDs, respectively.

In order to examine this possibility, a comparison is made with the bimodal height distribution of the dots shown in Fig. 7(c). Since edge-component dislocations are the

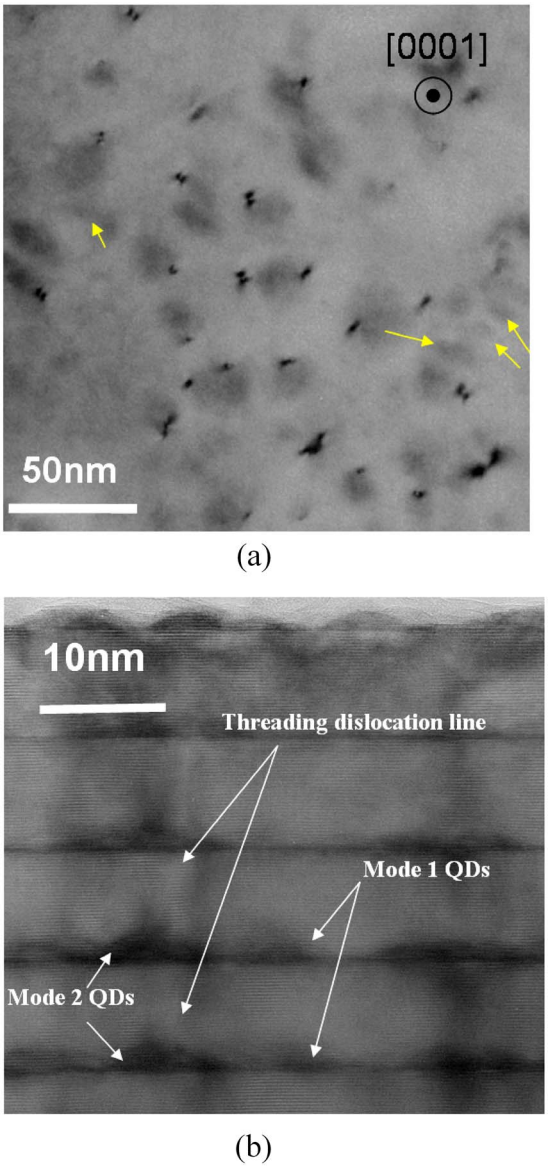

FIG. 10. (Color online) (a) Bright-field plan-view TEM image of GaN QDSL sample with 30 GaN stacks; (b) cross-sectional TEM image of same sample.

prevalent type of defects in this sample, the TD density can be reasonably estimated by directly counting the number of defects visible in plan-view diffraction-contrast images taken along the [0001] zone axis. By counting the number of dislocations and GaN QDs visible in larger-area plan-view TEM images, the density of dislocations with edge component is estimated to be 6.7×10^{10}/cm^2, while the QD density is estimated to be 8.5×10^{10}/cm^2. It should be noted that the QD density values for this sample estimated from the TEM images (8.5×10^{10}/cm^2) and from AFM results (8×10^{10}/cm^2) are similar. The ratio of the edge-component dislocation density (6.7×10^{10}/cm^2) to the total dot density (8.5×10^{10}/cm^2) is 79%. From the AFM height distribution of this sample, Fig. 7(c), the ratio of mode 2 dot density (6.3×10^{10}/cm^2) to the total dot density (8×10^{10}/cm^2) is 79%. The comparative analysis is summarized in Table I. The above observations and analysis suggest that the larger

Downloaded 21 Oct 2008 to 128.197.27.9. Redistribution subject to AIP license or copyright; see http://jap.aip.org/jap/copyright.jsp

TABLE I. Comparison of AFM and TEM measurements for GaN QDs.

AFM	Density (cm^{-2})	TEM	Density (cm^{-2})
Mode 1	1.7×10^{10}	···	···
Mode 2	6.3×10^{10}	TDs with edge component	6.7×10^{10}
Total dots	8×10^{10}	Total dots	8.5×10^{10}
Mode 2/Total	0.79	TDs/Total dots	0.79

and taller dots (mode 2) are preferentially associated with TDs while the smaller and shorter dots (mode 1) are located in TD-free regions.

C. Growth model for GaN QDs at high temperatures

Based on the AFM and TEM observations, as well as previous Ge/Si studies,[15–18] a model for the high-temperature growth of GaN QDs on AlN templates with high dislocation density is proposed. During the deposition of GaN on AlN, a layer of Ga metal is present on the surface due to the Ga-rich growth condition, and the growth is 2D [Fig. 11(a)]. When the growth is interrupted in vacuum after several MLs of GaN are deposited, the excess Ga is desorbed from the surface, as shown in Fig. 11(b). The strain energy will then be elastically relaxed by the 2D to 3D transition. In the early stages of GaN QD formation, the dots are likely to be preferentially located at the threading dislocations due to their ready availability as nucleation sites [see Fig. 11(c)], although dots may also nucleate in areas that are free of dislocations. In the ripening stage of GaN QD formation, dot growth is likely to be controlled by the competitive capture of diffusing adatoms by the various available surface sinks.[18] The TDs will act as adatom sinks that alter the surface diffusion and nucleation processes significantly. Smaller dots (mode 1) which are coherently strained and defect-free will grow more slowly than larger dots (mode 2), which are associated with dislocations, because of the energy cost associated with addition of atoms to a strained lattice [Fig. 11(d)].

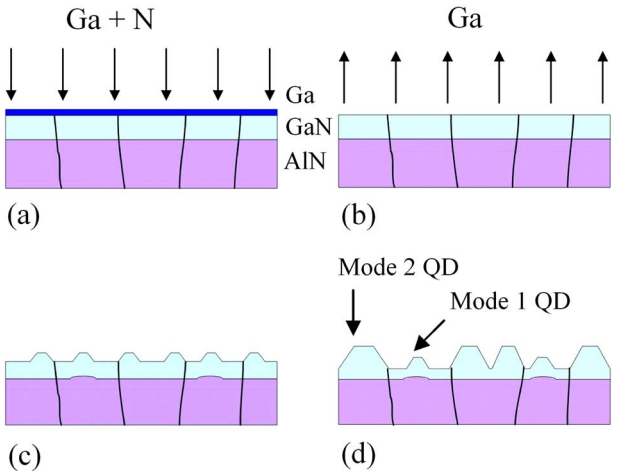

FIG. 11. (Color online) Growth model for GaN QDs grown on AlN buffer with high dislocation density. (a) During GaN deposition in the "modified Stranski-Krastanov" growth mode, an adlayer of Ga is present on the GaN surface to keep surface 2D. (b) When growth is stopped in vacuum, excess Ga on GaN surface is evaporated to expose GaN surface in vacuum. (c) In the early stage of GaN QD formation, dots will be preferentially located near threading dislocations due to lower energy. Dots will also nucleate in areas that are free of dislocations. (d) In the ripening stage of GaN QDs, dots close to dislocations (mode 2) will grow faster with larger height and diameter than dots located in area free of dislocations (mode 1). Mode 1 QDs are coherently strained with the AlN layer underneath, while mode 2 QDs are partially relaxed.

It is well known that the energy barrier for nucleation is reduced by the free energy of a defect.[19] It was reported for the Ge/Si system that coherent islands required substrate deformation over a range of approximately two times the island diameter.[16,20] When the GaN coverage is increased, the dot density becomes higher and dots will be closer to each other. For higher GaN coverage, it is thus more difficult to form coherent islands through AlN spacer deformation. More islands will be partially relaxed by misfit dislocations instead of the strain of the AlN spacer layer and their energy barrier to further growth is removed. Consequently, mode 2 dots will become more predominant with increasing GaN coverage (Fig. 3). However, besides GaN QD coverage, the high substrate temperature employed during the growth should also play a role since it facilitates the coalescence of smaller dots into larger ones. Furthermore, the observation that larger dots appear to nucleate next to the TDs with edge component suggests that the dislocations in the starting template may also play a role for the dominance of mode 2.

For mode 1 dots, the partial strain in the dots may be relaxed by the deformation of the underlying AlN barrier.[16] Because the dislocation density is smaller for the 30-stack GaN QDSL sample, there will be more mode 1 dots that are coherently strained with the AlN compared with the 4-stack GaN QDSL sample. This is consistent with the GID results shown in Fig. 9, where the peak due to AlN in the 30-stack GaN QDSL sample deviates from its unstrained $(10\bar{1}0)$ position, indicating that the AlN spacer is more strained than in the 4-stack GaN/AlN QDSL sample.

IV. CONCLUSIONS

In conclusion, we report the study of GaN/AlN QDSLs grown by MBE at relatively high temperature (770 °C) in the modified SK mode. The height of the dots showed a bimodal distribution with the larger and taller dots (mode 2) becoming more dominant with greater GaN monolayer coverage. The density of quantum dots increased with the amount of coverage and saturated at 2×10^{11} dots/cm^2. For the GaN coverage of 4 ML, mode 1 dots (smaller height) became more prominent as the number of stacks in the superlattice is increased. TEM studies suggested that the larger dots were most often nucleated at edge-type dislocations, whereas smaller dots were usually located in dislocation-free regions. GISAXS studies were used to estimate the average lateral deviation and the vertical correlation length between QD positions for successive layers to be 1.4 nm and 190 nm, respectively. A growth model has been proposed for the GaN QDs grown on AlN layers with high density of threading dislocations: for less than 5 ML GaN coverage, those dots which are preferentially nucleated at dislocations grow faster than those nucleated away from dislocations, possibly due to the energy barrier induced by the dislocations in the AlN

Downloaded 21 Oct 2008 to 128.197.27.9. Redistribution subject to AIP license or copyright; see http://jap.aip.org/jap/copyright.jsp

interlayer. When the GaN coverage increases, the QD density increases and the dots become closer laterally. The interaction of QDs changes the strain field and potentially helps mode 1 dots overcome the energy barrier and grow larger.

ACKNOWLEDGMENTS

This work was partially supported by DOE Grant No. RF-06-PRD-001 (subcontract from the University of Nevada, Las Vegas), by DOE Grant No. DE-FG02-03ER46037, and by ONR Grant No. N-00014-04-1-0020. We acknowledge use of facilities in the John M. Cowley Center for High Resolution Electron Microscopy at Arizona State University. Some of the data for this study were measured at beamline X21 of the National Synchrotron Light Source (NSLS). Financial support from the NSLS comes principally from the Offices of Biological and Environmental Research and of Basic Energy Sciences of the U.S. Department of Energy.

[1]C. Adelmann, B. Daudin, R. A. Oliver, G. A. D. Briggs, and R. E. Rudd, Phys. Rev. B **70**, 125427 (2004).
[2]N. Gogneau, D. Jalabert, E. Monroy, T. Shibata, M. Tanaka, and B. Daudin, J. Appl. Phys. **94**, 2254 (2003).
[3]J. Brown, F. Wu, P. M. Petroff, and J. S. Speck, Appl. Phys. Lett. **84**, 690 (2004).
[4]J. Brault, S. Tanaka, E. Sarigiannidou, J.-L. Rouviere, B. Daudin, G. Feuillet, and H. Nakagawa, J. Appl. Phys. **93**, 3108 (2003).
[5]M. Arley, J. L. Rouviere, F. Widmann, B. Daudin, G. Feuillet, and H. Mariette, Appl. Phys. Lett. **74**, 3287 (1999).
[6]T. Xu, C. Thomidis, I. Friel, and T. D. Moustakas, Phys. Status Solidi C **2**, 2220 (2005).
[7]G. Renaud, R. Lazzari, C. Revenant, A. Barbier, M. Noblet, O. Ulrich, F. Leroy, J. Jupille, Y. Borensztein, C. R. Henry, J. P. Deville, F. Scheurer, J. Mane-Mane, and O. Fruchart, Science **300**, 1416 (2003).
[8]Q. Xie, A. Madhukar, P. Chen, and N. P. Kobayashi, Phys. Rev. Lett. **75**, 2542 (1995).
[9]G. S. Solomon, J. A. Trezza, A. F. Marshall, and J. S. Harris, Jr., Appl. Phys. Lett. **76**, 952 (1996).
[10]P. Schittenhelm, C. Engel, F. Findeis, G. Abstreiter, A. A. Darhuber, G. Bauer, A. O. Kosogov, and P. Werner, J. Vac. Sci. Technol. B **16**, 1575 (1998).
[11]G. Capellini, L. Di Gaspare, F. Evangelisti, E. Palange, A. Notargiacomo, C. Spinella, and S. Lombardo, Semicond. Sci. Technol. **14**, L21 (1999).
[12]J. L. Rouviere, J. Simon, N. Pelekanos, B. Daudin, and G. Feuillet, Appl. Phys. Lett. **75**, 2632 (1999).
[13]I. Kegel, T. H. Metzger, J. Peisl, J. Stangl, G. Bauer, and D. Smilgies, Phys. Rev. B **60**, 2516 (1999).
[14]V. Chamard, T. H. Metzger, E. Bellet-Amalric, B. Daudin, C. Adelmann, H. Mariette, and G. Mula, Appl. Phys. Lett. **79**, 1971 (2001).
[15]A. Sakai and T. Tatsumi, Phys. Rev. Lett. **71**, 4007 (1993).
[16]D. J. Eaglesham and M. Cerullo, Phys. Rev. Lett. **64**, 1943 (1990).
[17]Y.-W. Mo, D. E. Savage, B. S. Swartzentruber, and M. G. Lagally, Phys. Rev. Lett. **65**, 1020 (1990).
[18]M. Krishnamurthy, J. S. Drucker, and J. A. Venables, J. Appl. Phys. **69**, 6461 (1991).
[19]J. W. Christian, *The Theory of Transformation in Metals and Alloys I* (Pergamon, Oxford, 1981), p. 448.
[20]F. K. LeGoues, M. Copel, and R. M. Tromp, Phys. Rev. Lett. **63**, 1826 (1989).

Downloaded 21 Oct 2008 to 128.197.27.9. Redistribution subject to AIP license or copyright; see http://jap.aip.org/jap/copyright.jsp